Available online at www.sciencedirect.com
ScienceDirect
Physica A 371 (2006) 725–731
PHYSICA A
www.elsevier.com/locate/physa

Long-range dependence in North Atlantic sea level

S.M. Barbosa*, M.J. Fernandes, M.E. Silva

Departamento de Matemática Aplicada, Faculdade de Ciências da Universidade do Porto, Rua Campo Alegre, 689, 4160-007, Porto, Portugal

Received 15 February 2006; received in revised form 27 March 2006
Available online 2 May 2006

Abstract

Sea level is an important parameter in climate and oceanographic applications. In this work the scaling behavior of sea level is analyzed from time series of sea level observations. The wavelet domain is particularly attractive for the identification of scaling behavior in an observed time series. The wavelet spectrum from a scale-by-scale wavelet analysis of variance reproduces in the wavelet domain the power laws underlying a scaling process, allowing the estimation of the scaling exponent from the slope of the wavelet spectrum. Here the scaling exponent is estimated in the wavelet domain for time series of sea level observations in the North Atlantic: at coastal sites from tide gauges, covering 50 years of monthly measurements, and in the open ocean from satellite altimetry, covering 12 years of satellite measurements at 10 days intervals. Both tide gauge and altimetry time series exhibit scaling behavior. Furthermore, the degree of stochastic persistence is spatially coherent and distinct at the coast and in the open ocean. Near the coast, the stochastic structure of the sea level observations is characterized by long-range dependence with a moderate degree of persistence. Larger values of the scaling exponent, consistent with weaker persistence, are concentrated in the northern Atlantic. At mid-latitudes the stochastic dependence of sea level observations is characterized by strong persistence in the form of strong long-range and 1/f dependence.

Keywords: Sea level; Wavelet methods; Scaling; North Atlantic

1. Introduction

Long-range dependence was first noted in hydrology by H.E. Hurst from the study of the water levels of the Nile river as the tendency for a flood year to be followed by another flood year. The term "Joseph effect" was introduced to describe such temporal persistence, as an allusion to the seven years of Egyptian plenty followed by the seven years of famine in the biblical story of Joseph [1]. Time series exhibiting long-range dependence are characterized in the time domain by persistent autocorrelations, decaying as a power law, and in the frequency domain by high spectral content at frequency zero. Long-range dependent systems exhibit scale invariance (absence of a typical time scale) and are characterized by an autocorrelation function with a slow, hyperbolic decay, $C(k) \propto k^{-\gamma}$ and a spectral density function of the form $S(f) \propto f^{-\beta}$, $0<\beta<1$.

*Corresponding author. Tel.: +351 220 100 802; fax: +351 220 100 809.
E-mail address: susana.barbosa@fc.up.pt (S.M. Barbosa).

0378-4371/$ - see front matter © 2006 Elsevier B.V. All rights reserved.
doi:10.1016/j.physa.2006.03.046

Long-range dependence has been identified in a wide range of applications from DNA sequences [2] to finance [3]. The identification of long-range dependence in the climate system is motivated by the practical and physical implications of temporal persistence for forecasting, model assessment and characterization of climate variability. A number of studies have been devoted to the analysis of persistence features in time series of surface temperature. Koscielny-Bunde et al. [4] analyzed temperature records from continental stations and concluded for a similar "universal scaling law" for all stations with exponent $\beta\sim0.3$. However, analysis of the geographical pattern of scaling have concluded that both observations and model outputs of near surface temperature display distinct scaling laws for continental and maritime data: close to $1/f$ noise over the oceans, near white noise in the inner continents and with an exponent $\beta\sim0.3$ along the coastal transition regions [5,6]. Observations of sea surface temperature have been found to display $1/f$ (or flicker noise) behavior at mid-latitudes [7]. The $1/f$ spectrum of the ocean surface temperature at mid-latitudes can be explained by a simple vertical diffusion model with a shallow mixed layer on top of a deep ocean [8].

Sea level is a climate parameter not only closely related to temperature but also influenced by a large number of atmospheric and oceanographic phenomena, from atmospheric pressure and winds to tides and ocean currents. Sea level variations over the past 150–250 million years, inferred from deep-sea sediments, exhibit long-range dependence with $\beta\sim1$ [9]. In this work the temporal persistence in sea level is analyzed from direct sea level observations over the instrumental period, from tide gauges and TOPEX/Poseidon satellite altimetry mission, using a wavelet-based approach.

2. Methodology

Detrended fluctuation analysis (DFA) [10] is often used in the investigation of scaling behavior in geophysical time series. However, DFA may not be able to establish long-range persistence unambiguously [11,12]. An alternative approach is to analyze the scaling behavior of an observed time series in the wavelet domain.

The maximal overlap discrete wavelet transform (MODWT) is a highly redundant non-orthogonal transform that can be efficiently computed through a recursive pyramid algorithm [13,14]. The partial MODWT of level J for a time series X_t of length N yields $J+1$ transform vectors $\mathbf{W}_i \in \mathbb{R}^N, i=1,\ldots,J$ and $\mathbf{V}_J \in \mathbb{R}^N$, from $N\times N$ transform matrices $\mathscr{W}_j$ and $\mathscr{V}_J$. The vector $\mathbf{W}_j = \mathscr{W}_j\mathbf{X}$ contains the MODWT wavelet coefficients associated with changes on scale $\tau_j = 2^{j-1}\Delta t$ while the vector $\mathbf{V}_J = \mathscr{V}_J\mathbf{X}$ contains the MODWT scaling coefficients associated with scales of $\lambda_J = 2^J\Delta t$ and higher. The wavelet variance at scale τ_j, denoted by $v_X^2(\tau_j)$, represents the contribution to the total variability in X_t from changes at scale τ_j and is defined by $v^2(\tau_j) = V[\mathbf{W}_j]$. An unbiased estimator for the wavelet variance is given by [15,16]

$$\widehat{v}^2(\tau_j) = \frac{1}{M_j}\sum_{t=L_j-1}^{N-1} W_{j,t}^2, \tag{1}$$

where $L_j = (2^j-1)(L-1)+1$ is the width of the equivalent wavelet filter and $M_j = N-(2^j-1)(L-1)$ is the number of non-boundary MODWT coefficients for a time series of length N and a wavelet filter of width L. In practice boundary coefficients can be excluded by establishing a "brick-wall" boundary condition which prohibits convolutions that extend beyond the ends of the time series [17]. The level J of the MODWT is set in practice equal to $J = integer[\log_2 N - \log_2(2L+1)]$ in order to ensure that enough wavelet coefficients, not affected by boundary conditions, remain for the computation of the wavelet variance.

Discrete wavelet analysis is particularly useful to handle scaling behavior in a time series. The wavelet variance of a process over all dyadic scales j constitutes a second order description of the process through a "wavelet spectrum," providing a summary of the spectral density function with large values of j corresponding to low frequencies and small values of j to high frequencies. The wavelet spectrum from a wavelet scale-based analysis of variance allows the detection and estimation of long-range dependence in a time series since it reproduces in the wavelet domain the power laws underlying the scaling processes [18]. The identification of long-range dependence from the wavelet spectrum is based on the relation between wavelet variance and scale,

which is approximately described by a power law and therefore, in logarithmic coordinates, by a straight line with slope α

$$\log(\hat{\nu}^2(\tau_j)) \sim \xi + \alpha \log(\tau_j), \quad j = l, l+1, \ldots, J, \quad l \geqslant 2. \tag{2}$$

The slope α can be estimated from the MODWT-based wavelet spectrum by weighted least squares [14]. The exponent β of a long-range dependent process is related to the slope α of the wavelet spectrum by

$$\beta = \alpha + 1. \tag{3}$$

3. Data

Two types of available sea level measurements are analyzed in this study: sea level observations from tide gauges, constrained to coastal locations, and satellite altimetry observations from the TOPEX/Poseidon mission, on a nearly global spatial scale.

Tide gauge data in the form of monthly time series are obtained from the permanent service for mean sea level (PSMSL) database [19] for 16 stations in the North Atlantic with long ($\gtrsim 50$ years) and continuous records (gaps <1 year, missing values $<2.5\%$) of relative sea level heights (Fig. 1).

Satellite altimetry data in the form of merged geophysical data records (GDR-Ms) products are obtained from AVISO [20]. The dataset considered covers nearly 12 years from September 1992 to March 2005 (cycles 1–460) at intervals near 10 days (corresponding to the repeat period of the satellite). The satellite ground-tracks, illustrating the spatial distribution of altimetry measurements for a cycle of data, are represented in Fig. 1. Time series of sea level anomalies (SLA) on a regular $2.5^\circ \times 2.5^\circ$ grid over the North Atlantic are obtained by applying instrumental and state-of-art geophysical corrections to the TOPEX altimetry measurements and by removing the mean sea surface from the GSFC00.1 model [21]. The methodology adopted for the computation of sea level anomalies is similar to the one described in Ref. [22]. A total number of 603 time series with 460 observations each are derived for the study region.

Seasonal signals are the dominant features in time series of sea level observations. Since the presence of periodic features influences the identification of scaling behavior, even in the wavelet domain [23], the seasonal

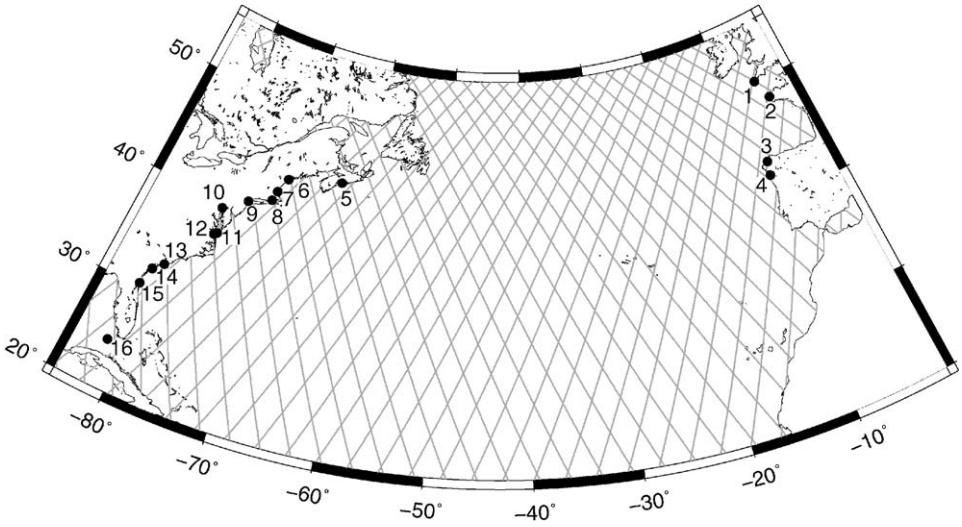

Fig. 1. Study area with satellite tracks (gray lines) and tide gauge locations: 1—Newlyn; 2—Brest; 3—Coruna; 4—Vigo; 5—Halifax; 6—Portland; 7—Boston; 8—Newport; 9—New York; 10—Baltimore; 11—Kiptopeke; 12—Hampton; 13—Charleston; 14—Fort Pulaski; 15—Mayport; 16—Key West.

signal is estimated by a sinusoidal regression at the annual and semi-annual frequencies and removed from all sea level series.

4. Results

A level $J = 6$ MODWT is carried out for each sea level series using a Daubechies wavelet filter of length $L = 4$ with brick-wall boundary conditions [24] . The MODWT yields a scale-based decomposition of the time series in the wavelet domain as illustrated in Fig. 2 for an altimetry series. The wavelet variance $v^2(\tau_j)$ is estimated for each scale j from the resulting MODWT wavelet coefficients (Eq. (1)) and plotted versus scale on a log10–log10 plot along with the corresponding 95% confidence intervals (Fig. 3). The slope of the wavelet spectrum (Eq. (2)) is computed by weighted least squares [14]. Estimates for the exponent β are obtained directly from the slope of the wavelet spectrum α (see Eq. (3)).

The resulting estimates of the scaling exponent β from the tide gauge and satellite altimetry series are displayed in Fig. 4. Table 1 contains the values of β for the tide gauge records. The values of the scaling exponent exhibit large scale-spatial coherency with a clear latitudinal dependency. At higher latitudes, sea level exhibits scaling behavior consistent with white noise ($\beta \sim 0$) and short-range dependence ($\beta \lesssim 0$) while at mid-latitudes the values of the scaling exponent are larger, corresponding to strong long-range dependence and 1/f or flicker noise ($\beta \sim 1$). The coastal sites seem to follow the sea level oceanic pattern, with lower values of β for

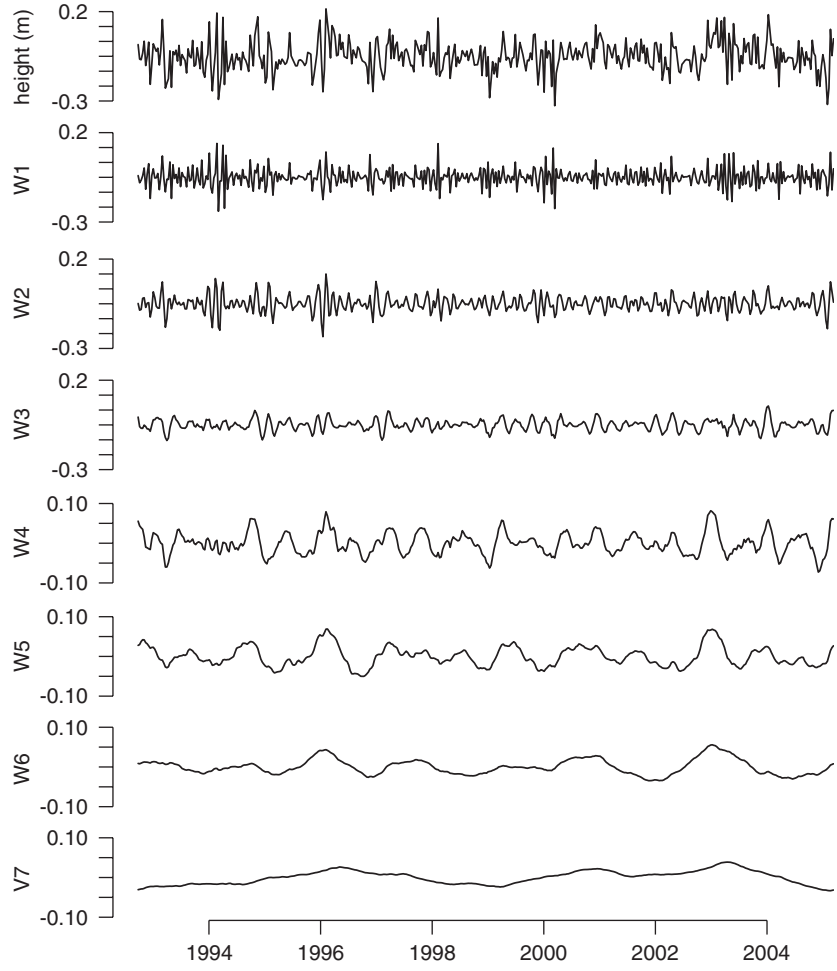

Fig. 2. Maximal overlap discrete wavelet transform (MODWT) for a satellite altimetry time series of sea level anomalies. From top to bottom: de-seasoned time series and MODWT components. Units of vertical scales are in meters.

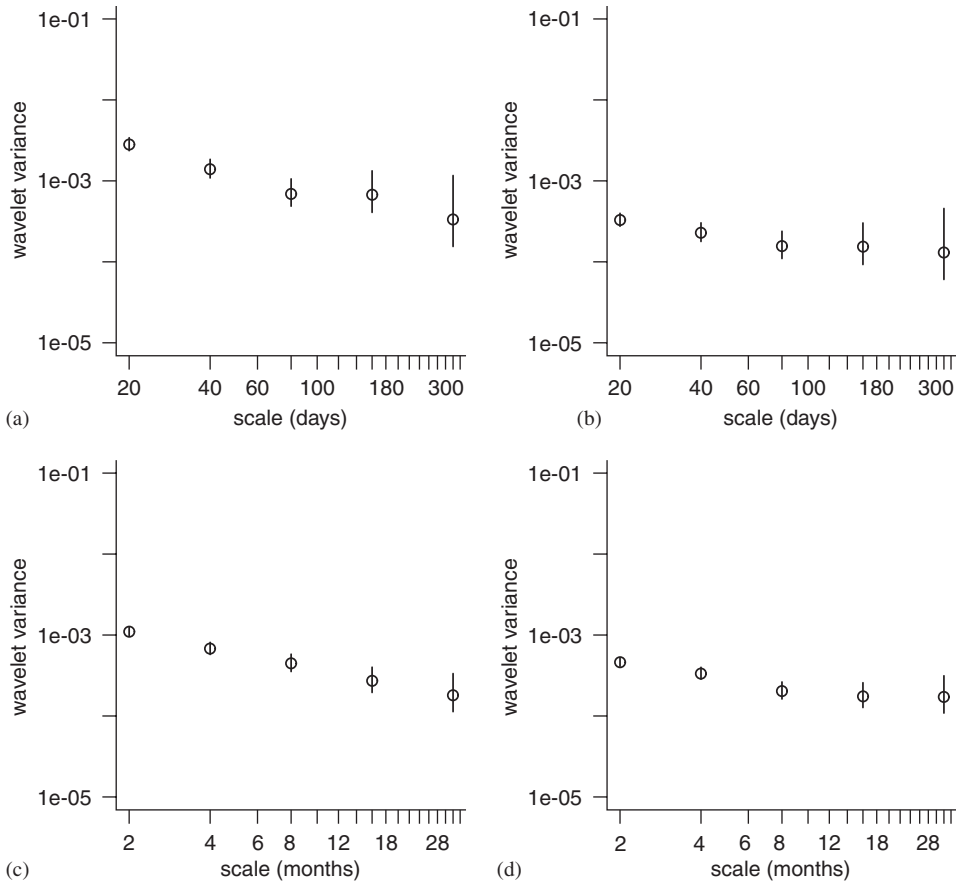

Fig. 3. Wavelet spectrum for typical sea level series of altimetry (a–b) and tide gauge (c–d) sea level observations: (a) gridpoint −52.5E, 52.5N; (b) gridpoint −17.5E, 7.5N; (c) Newlyn tide gauge; (d) Key West tide gauge.

the northern stations (Newlyn, Brest, Halifax) and larger values, consistent with long-range dependent behavior, for the mid-latitude stations ($\beta \gtrsim 0.5$).

5. Conclusions

Assessment of scaling behavior from an observed time series is particularly appealing in the wavelet domain. The wavelet variance provides a summary of the spectral density function in the wavelet domain enabling the estimation of the scaling exponent β from the slope of the wavelet spectrum. The wavelet approach is blind to any superimposed polynomial trends and thus is particularly attractive for distinguishing between stochastic persistence and deterministic features in an observed series, giving additional insight on the underlying stochastic structure.

Our results indicate that sea level series from tide gauge and satellite altimetry measurements in the North Atlantic exhibit scaling behavior. Furthermore, the degree of persistence as measured by the scaling exponent β exhibits a spatial-coherent pattern over the North Atlantic. Lower values of β, corresponding to short-range dependence and weak persistence are concentrated in the northern Atlantic. At mid-latitudes the values of β are higher, corresponding to strong persistence in the form of long-range dependence and $1/f$ non-stationarity. Near the coast, the stochastic structure of the sea level observations is characterized by long-range dependence with a moderate degree of persistence. These results for sea level are consistent with distinct scaling laws found in sea surface temperature observations and model outputs [6,5] which also indicate distinct scaling regimes near the coast and in the open ocean.

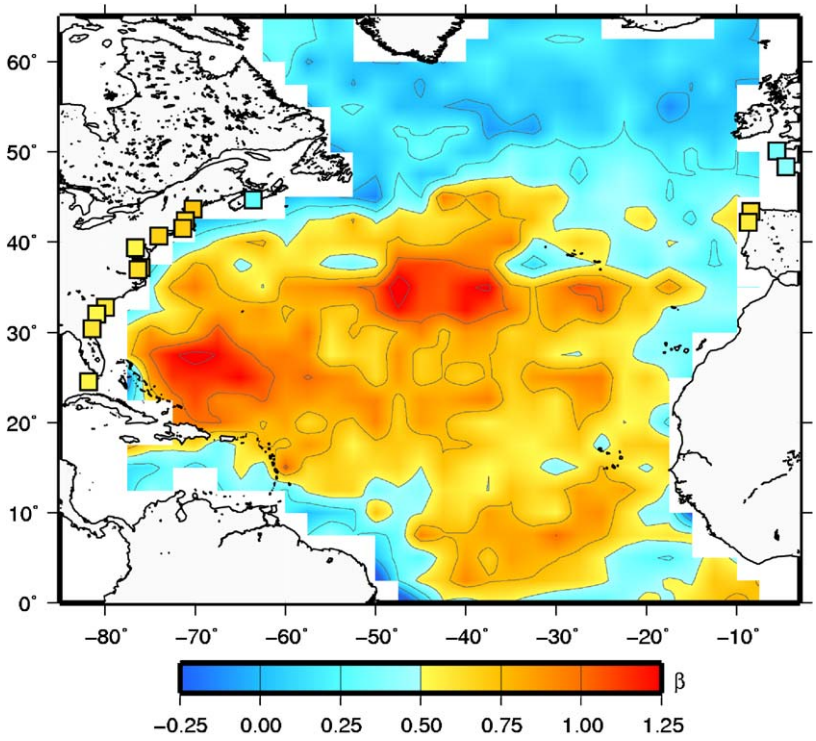

Fig. 4. Scaling exponent (β) for sea level series in the North Atlantic from satellite altimetry (open ocean) and tide gauges (at the coast, □).

Table 1
Estimates of the scaling exponent β for each tide gauge record

	β		β
Newlyn	0.34	New York	0.68
Brest	0.41	Baltimore	0.53
Coruna	0.62	Kiptopeke	0.67
Vigo	0.57	Hampton	0.63
Halifax	0.28	Charleston	0.59
Portland	0.72	Fort Pulaski	0.53
Boston	0.64	Mayport	0.60
Newport	0.70	Key West	0.54

Acknowledgement

This work has been supported by program POCTI through the Centro de Investigação em Ciências Geo-espaciais (CICGE) of the Faculty of Science, University of Porto.

References

[1] B.B. Mandelbrot, J.R. Wallis, Water Resour. Res. 4 (1968) 909–918.
[2] S.V. Buldyrev, A.L. Goldberger, S. Havlin, R.N. Mantegna, M.E. Matsa, C.-K. Peng, M. Simons, H.E. Stanley, Phys. Rev. E 51 (1995) 5084–5091.

[3] M. Henry, P. Zaffaroni, in: P. Doukhan, G. Oppenheim, M.S. Taqqu (Eds.), Theory and Applications of Long Range Dependence, Birkhauser, Boston, 2003, pp. 417–438.
[4] E. Koscielny-Bunde, A. Bunde, S. Havlin, H.E. Roman, Y. Goldreich, H.-J. Schellnhuber, Phys. Rev. Lett. 81 (1998) 729–732.
[5] K. Fraedrich, R. Blender, Phys. Rev. Lett. 90 (2003) 108501.
[6] R. Blender, K. Fraedrich, Geophys. Res. Lett. 30 (2003) 1769.
[7] R.A. Monetti, S. Havlin, A. Bunde, Physica A 320 (2003) 581–589.
[8] K. Fraedrich, U. Luksch, R. Blender, Phys. Rev. E 70 (2004) 037301.
[9] A.T. Hsui, K.A. Rust, G.D. Klein, J. Geophys. Res. 98 (1993) 21,963–21,968.
[10] C.-K. Peng, S.V. Buldyrev, A.L. Goldberger, S. Havlin, M. Simons, H.E. Stanley, Phys. Rev. E 47 (1993) 3730–3733.
[11] P. Talkner, R.O. Weber, Phys. Rev. E 62 (2000) 150–160.
[12] D. Maraun, H.W. Rust, J. Timmer, Nonlinear Process. Geophys. 11 (2004) 495–503.
[13] D.B. Percival, H. Mojfeld, J. Am. Stat. Assoc. 92 (1997) 868–880.
[14] D.B. Percival, A. Walden, Wavelet Methods for Time Series Analysis, Cambridge University Press, Cambridge, 2000.
[15] D.B. Percival, Biometrika 82 (1995) 619–631.
[16] A. Serroukh, A.T. Walden, D.B. Percival, J. Am. Stat. Assoc. 95 (2000) 184–196.
[17] R.W. Lindsay, D.B. Percival, D.A. Rothrock, IEEE Trans. Geosci. Remote 34 (1996) 771–787.
[18] P. Abry, P. Flandrin, M.S. Taqqu, D. Veitch, in: P. Doukhan, G. Oppenheim, M.S. Taqqu (Eds.), Theory and Applications of Long Range Dependence, Birkhauser, Boston, 2003, pp. 527–556.
[19] P.L. Woodworth, R. Player, J. Coastal Res. 19 (2003) 287–295.
[20] AVISO User Handbook, AVI-NT-02-101-CN, 1996.
[21] Y.M. Wang, J. Geophys. Res. 106 (2001) 31167–31174.
[22] M.J. Fernandes, S.M. Barbosa, C. Lazaro, Sensors 6 (2006) 131–163.
[23] D. Markovic, M. Koch, Geophys. Res. Lett. 32 (2005), doi:10.1029/2005GL024069.
[24] I. Daubechies, Commun. Pure Appl. Math. 41 (1988) 909–996.